© 1999 The Chemical Society of Japan

Bull. Chem. Soc. Jpn., *72*, 1213—1217 (1999)

Electronic Spectra of the Electrogenerated 1,4-Benzoquinone π-Dianion and the Strongly Hydrogen-Bonded Charge-Transfer Complex with Methanol

Noriko Okumura and Bunji Uno*

Gifu Pharmaceutical University, Mitahora-higashi, Gifu 502-8585

(Received November 24, 1998)

Electronic spectra of the active π-electronic dianion of 1,4-benzoquinone and its hydrogen-bonded complex with CH_3OH, generated at sequential electroreduction steps, have been discussed from the points of view of the observation techniques and n–σ charge-transfer interaction of the dianion with a weak hydrogen donor. An improved method involving rapid circulation of the electrolyzed solution via a photodiode array detector to avoid comproportionation and side reactions was used for successful measurements of the clear spectra resulting from the dianion generation. CNDO/S-CI calculations well reproduced the longest-wavelength band observed for the dianion, assigning to the benzenoid $^1B_{3u} \leftarrow {}^1A_g$ band under D_{2h} symmetry. The hydrogen-bonding interaction of the 1,4-benzoquinone dianion with CH_3OH allows the $^1B_{3u} \leftarrow {}^1A_g$ band to be blue-shifted. This behavior has been well explained in terms of the strong n–σ type charge-transfer interaction of the dianion with CH_3OH. These results have been extensively discussed with regard to coupled electron and proton transfer reactions in the quinone–hydroquinone redox system.

Great interest is currently devoted to the π-dianions of organic molecules generated by sequential electroreduction and two-electron reduction with an alkali metal, with regard to the interaction with cationic species and hydrogen donors,[1—3] the electronic multiplicity,[4—7] the conformational properties,[8,9] and the reactivity.[10—12] The electrochemical behavior of the dianion generation has been well-documented in terms of their intrinsic chemical interest and biological importance.[13—15] The dianions of quinones are of especial interest in view of the key biological functions of coupled electron and proton transfer reactions.[3,8,16] In our previous paper have been discussed for the first time the problem of how active the *p*-quinone π-dianions are as proton acceptors, with the aid of electrochemical evaluation of the formation constants for the two-point hydrogen-bonded complexes with CH_3OH.[1] After that, hydrogen bonding and protonation effects in electrochemistry of quinones in aprotic media have been extensively discussed on the basis of electrochemical and vibration spectral measurements, and molecular orbital calculations with regard to the biological importance.[3,8]

Spectroscopic measurements are currently done to characterize the organic dianions.[2,4—9,11] Most workers have documented dependence of the NMR behavior upon the structure and the electronic states of the dianions generated by the reduction with an alkali metal.[4—7,9,11] Spectral measurements for the electrochemically generated dianions are of great importance in gaining deeper insight into the coupled electron-transfer process. Recently, resonance Raman and FTIR spectra were adapted to analyze the conformation and the electronic states of the electrochemically two-electron reduced quinones.[8] Spectroelectrochemistry in the ultraviolet and visible regions is indispensable to characterize the dianions and to analyze the interaction with additives as it has contributed the research for radicals. However, the spectral investigation is surprisingly limited to the stable dianions involving CN groups and halogens such as TCNQ and 2,3-dichloro-5,6-dicyano-1,4-benzoquinone, mainly due to instability which comes from comproportionation and side reactions.[2] In this paper we have devised a more suitable and simpler method for spectroelectrochemical observation of the dianions than those reported in the literature such as the pulse electrolysis stopped-flow, column-electrolysis and thin-layer electrolysis methods.[16—18] Discussion has been extended to spectral characteristics of the 1,4-benzoquinone (BQ) dianions and the hydrogen-bonded complex with CH_3OH. As a part of our continuing studies on active organic π-dianions,[1,19] the strong n–σ charge-transfer interaction of BQ^{2-} with a weak proton donor is documented on the basis of these spectral data and the CNDO/S-CI calculation results.

Experimental

Spectroelectrochemical and Electrochemical Measurements. Controlled-potential electrolysis was done in a bulk electrolysis cell of 100 dm^3, with a three-electrode system consisting of a reticulated vitreous carbon working electrode available from BAS, Co., an $Ag/AgNO_3$ (in CH_3CN) reference electrode, and a platinum wire counter electrode, illustrated in Fig. 1. The reference electrode was sealed by Vycor glass, and the counter electrode was separated from the bulk solution by a Vycor frit. A Hokuto Denko HA-501 potentiostat was used for the electrolysis, the electrode potential being set at sufficiently negative values to generate the anion radical and dianion species in consideration of the cyclic voltammograms (CV). A Shimadzu SPD-M10A photodiode array detector with the optical

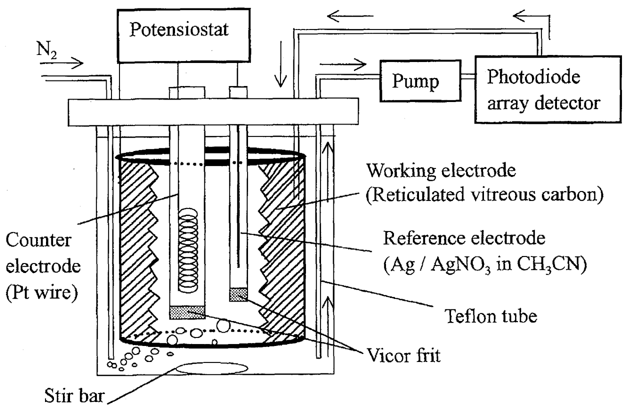

Fig. 1. Schematic diagram of the rapid circulation system consisting of a controlled-potential electrolysis cell, a potensiostat, and a photodiode array detector equipped with a personal computer.

path length of 1.0 cm equipped with a Gateway P5-100 personal computer was used for the spectral observation. The flow-type detector was connected with the electrolysis cell via a Shimadzu LC-10AD pump by Teflon® tubes of 0.8 mm inner diameter, in which the electrolyzed solution was circulated at a fast flow rate of 5 dm^3 min^{-1}, as shown in Fig. 1. N_2 gas was sufficiently bubbled into the sample solution before electrolysis to remove the dissolved oxygen. During the measurements the sample solution was vigorously stirred and bubbled with N_2 gas without exposure to an atmosphere. CV measurements were done with a BAS 100B electrochemical workstation, using a three-electrode system consisting of a glassy carbon working electrode, a platinum wire counter electrode, and an Ag/AgNO$_3$ (in CH$_3$CN) reference electrode.

Chemicals and Solvents. BQ was commercially available from Nacalai Tesque, Inc., and was purified by repeated sublimation under reduced pressure, then once again just before use.[20] CH$_3$OH and CH$_3$CN of spectrograde purity were purchased form Nacalai Tesque, Inc., and was dried over molecular sieves (3A) for more than 2 d and then carefully distilled. Tetrapropylammonium perchlorate (TPAP) was used as a supporting electrolyte for CH$_3$CN, being recrystallized twice from methanol and then dried in a high vacuum before use.[13]

Molecular Orbital (MO) Calculations. Semiempirical CNDO/S-CI calculations were done to clarify the spectral characteristics and to analyze the electronic states of BQ, BQ^{2-} and the hydrogen-bonded complexes with CH$_3$OH. The parameters necessary for the calculations were taken from the literature of Jaffé's group and others.[21—26] Two-center repulsion integrals were evaluated using the Nishimoto–Mataga equation.[27] Only the one-electron transition was taken into account for calculations of the configuration interaction (CI). Molecular geometries of BQ, BQ^{2-}, and their hydrogen-bonded complexes with CH$_3$OH used for the calculations were those optimized by HF/6-31G(d) calculations.

Results and Discussion

Observation of the Electronic Spectrum of Electrogenerated BQ^{2-}. It is well-known that sequential electroreduction of BQ affords BQ^- and BQ^{2-} in aprotic media such as CH$_3$CN, showing two reversible waves on the cyclic voltammograms. The half-wave reduction potentials were evaluated as −0.50 V (vs. Ag/AgNO$_3$ (in CH$_3$CN)) for the redox couple of BQ/BQ^-, and −1.07 V for the BQ^-/BQ^{2-} couple. BQ were also easily one-electron reduced in the bulk electrolysis cell at the applied potential of −0.9 V, and the absorption spectra of BQ systematically changed with the BQ^- generation, giving clear isosbestic points, as is shown in Fig. 2a. The characteristic bands of BQ^- were intensified in the beginning of the electrolysis, and the spectra changed no longer with the decrease in the cathode current for electrolysis, indicating the complete conversion into the anion radical. The stability of BQ^- allows the absorbance of the band to be unreduced for a long time after the electrolysis is stopped. Next, the spectral change with the BQ^{2-} generation

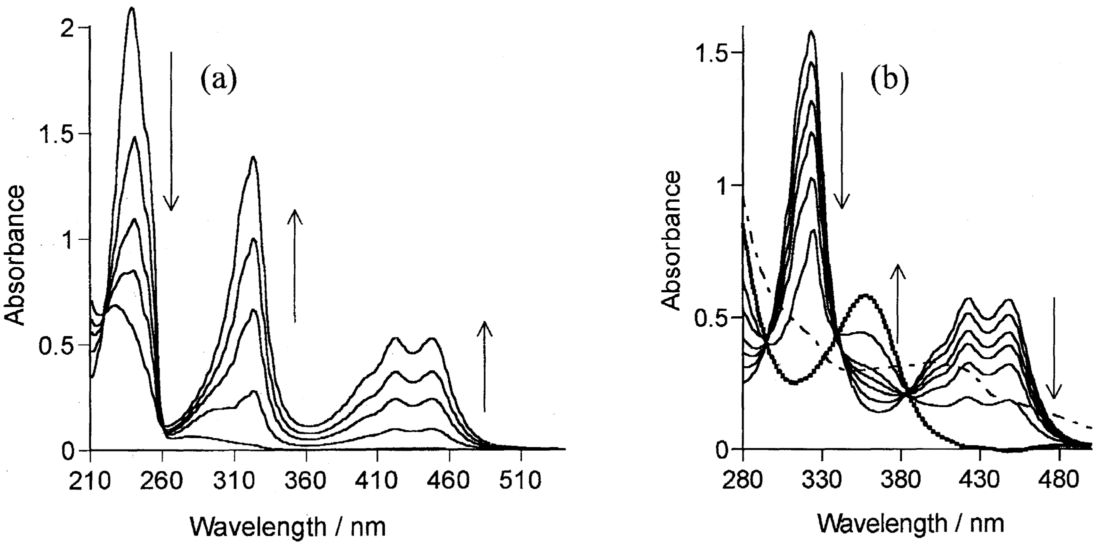

Fig. 2. Spectral change of BQ with electrolysis for the reaction of $BQ + e^- \rightarrow BQ^-$ (a) and $BQ^- + e^- \rightarrow BQ^{2-}$ (b). The sample concentration is 1.22×10^{-4} mol dm^{-3} in CH$_3$CN. The spectrum denoted by a dotted line in Fig. 2(b) corresponds to BQ^{2-} itself, calculated from the decrease in the absorbance of the 420 nm band of BQ^-. A dashed line in Fig. 2(b) denotes the spectra obtained after long electrolysis time. See the text for details.

has been observed at the applied potential of -2.5 V, showing clear isosbestic points, as shown in Fig. 2b. An increase in absorbance at 358 nm is observed with electrolysis time, corresponding to the BQ^{2-} generation. When the electrolysis is stopped, BQ^{2-} is quenched, probably due to the reoxidation by O_2 in minute quantity in solutions and the comproportionation reaction with the neutral species. It is difficult to record the systematic spectral change for the BQ^{2-} generation with electrolysis time without circulation at a flow rate rapider than 5 $dm^3\ min^{-1}$ and vigorous stirring of the sample solution. The important points for measuring the spectra of the electrogenerated active dianions with a flow system are therefore to complete the reduction quickly and effectively, and to quickly lead the electrolyzed solution into the optical cell without exposing it to an atmosphere. Rapid circulation of the electrolyzed solution via a photodiode array detector is suitable for this purpose. The prolonged electrolysis time, however, allows the spectra to get out of the isosbestic points as denoted by a dashed line in Fig. 2b, being indicative of resulting from the side reactions. The standard flow and column electrolysis methods as far as we used them gave only the similar spectra without isosbestic points, which were in agreement with the published spectrum for BQ.[2—8] These spectra may arise from the quinhydrone formation due to incomplete reduction and an unsuspected trace of moisture contaminating the solution during electrolysis. Although this method did not give the spectrum of BQ^{2-} itself observed for the completely electrolyzed solutions, the systematic change in the spectra allowed it to be calculated from the decrease in absorbance of the 420 nm band of BQ^{-}, as denoted by a dotted line in Fig. 2b.

Electronic Spectrum of the Strongly Hydrogen-Bonded Complex of BQ^{2-} with CH_3OH. In our previous papers it has been electrochemically and theoretically demonstrated that BQ^{2-} forms two-point hydrogen-bonded complexes with CH_3OH in CH_3CN.[1] The rapid circulation technique has been used for the spectral measurements of the hydrogen-bonded complex of BQ^{2-} with CH_3OH. The same spectral change with electrolysis time as those in Fig. 2 was observed on an addition of various concentrations of CH_3OH to the BQ solutions. The spectra corresponding to BQ^{2-} itself were estimated in the same manner as mentioned above. It has been found that the 358 nm band of BQ^{2-} is blue-shifted, depending upon the concentration of CH_3OH. Figure 3 shows the spectra of BQ^{2-} in the absence and in the presence of 1.23 $mol\ dm^{-3}$ CH_3OH. The CH_3OH concentration is enough to yield the two-point hydrogen-bonded complexes of all the BQ^{2-} molecules, judging from the observed formation constant previously reported.[1] The spectrum of B therefore corresponds to the hydrogen-bonded complex itself. We have safely said that the hydrogen bond to BQ^{2-} is characterized as the blue shift in the BQ^{2-} spectra, which is analogous to the case of the intramolecular charge-transfer π–π^* bands[28] and n–π^* bands.[29] Table 1 lists the spectral data of BQ^{2-} and the hydrogen-bonded complexes. It is clearly found that the absorption maximum of the BQ^{2-}–$(CH_3OH)_2$ complex is in consonance with that of BQ^{2-} generated by deprotonation in C_2H_5OH, and appears a wavelength longer than that of BQ^{2-} in water.[8,30] These spectral data clearly show that degree of the blue shift indicates the strength of hydrogen bonding to BQ^{2-}.

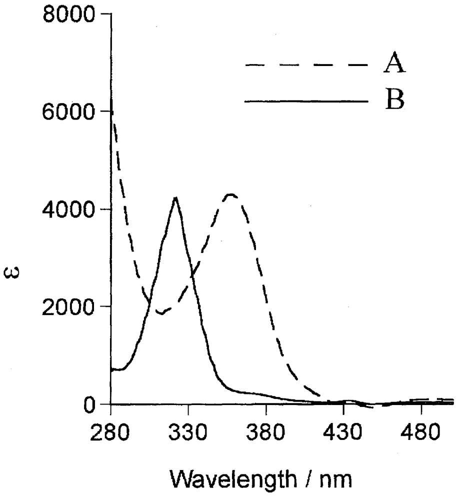

Fig. 3. Electronic spectra of BQ^{2-} (A) and the hydrogen-bonded complex with CH_3OH (B). These spectra were observed for the electrolyzed solutions in the absence of CH_3OH (A) and in the presence of 1.23 $mol\ dm^{-3}$ CH_3OH (B). See the text for the details.

Table 1. Absorption Maxima of BQ^{2-} and the Hydrogen-Bonded Complex with CH_3OH in CH_3CN, and BQ^{2-} in C_2H_5OH and H_2O

Compounds	Solvent	λ/nm
BQ^{2-}	CH_3CN	358
BQ^{2-}–$(CH_3OH)_2$	CH_3CN	322
BQ^{2-} [a]	C_2H_5OH	323[b]
BQ^{2-} [c]	H_2O	316[d]

a) Generated by deprotonation of BQH_2 in C_2H_5OH. b) Data from Ref. 30. c) Generated by deprotonation of BQH_2 in H_2O. d) Data from Ref. 8.

CNDO/S-CI Calculations for BQ^{2-} and the Hydrogen-Bonded Complex. Table 2 lists the spectral data for BQ, BQ^{2-}, and the hydrogen-bonded complex observed and calculated by the CNDO/S-CI calculation method. The longest wavelength band of BQ^{2-} is assigned to the $^1B_{3u}\leftarrow{}^1A_g$ transition corresponding to the benzenoid ^1L_b state with a transition moment along the x-axis under D_{2h} symmetry, mainly contributed from the b_{1g}-HOMO$\rightarrow a_u$-LUMO electronic configuration. This indicates that the BQ^{2-} prefers the benzenoid structure rather than the quinonoid form, which agrees with the optimized geometry calculation and the resonance Raman spectroscopic results.[1,8] The benzenoid band of BQ^{2-} is regarded as red-shifted by the substituent effect of a strongly electron-donating substituents such as the two p-(dimethylamino) groups on the ^1L_b band of benzene in consideration of the observed absorption maximum and the calculated HOMO→LUMO nature.[31]

Next, discussion was extended to the hydrogen-bonding effect on the BQ^{2-} spectra. The CNDO/S-CI calculations

Table 2. Spectral Data and CNDO/S-CI Calculation Results for the Longest Wavelength Bands of BQ, BQ^{2-}, and Their Hydrogen-Bonded Complexes with CH_3OH

	Observed[a)]	Calculated			
Compounds	E/eV (λ/nm)	E/eV (λ/nm)	f[b)]	CI(%)[c)]	Assignment[d)]
BQ	5.12 (242)	5.34 (232)	0.82	$92(b_{1u} \rightarrow b_{3g}), 5(b_{2g} \rightarrow a_u)$	$^1B_{2u} \leftarrow {}^1A_g$
$BQ–(CH_3OH)_2$	5.10 (243)	5.36 (231)	0.87	$93(b_{1u} \rightarrow b_{3g}), 5(b_{2g} \rightarrow a_u)$	$^1B_{2u} \leftarrow {}^1A_g$
BQ^{2-}	3.46 (358)	3.47 (357)	0.17	$93(b_{3g} \rightarrow a_u), 5(b_{2g} \rightarrow b_{1u})$	$^1B_{3u} \leftarrow {}^1A_g$
$BQ^{2-}–(CH_3OH)_2$	3.85 (322)	3.79 (327)	0.16	$91(b_{3g} \rightarrow a_u), 9(b_{2g} \rightarrow b_{1u})$	$^1B_{3u} \leftarrow {}^1A_g$

a) Values at the maximum intensity in CH_3CN. b) Oscillator strengths. c) For example, $(b_{1u} \rightarrow b_{3g})$ means a singly excited configuration from the b_{1u} filled π-MO to the b_{3g} unoccupied π-MO. d) Under D_{2h} symmetry.

reproduced the experimental blue shift with hydrogen-bond formation, as is seen from Table 2. The calculations furthermore provided clear-cut evidence for the blue shift in the BQ^{2-} spectra by hydrogen bonding. Figure 4 shows the calculated MO's relevant to the electronic transitions concerning the BQ and BQ^{2-} bands. The origin of the blue shift upon hydrogen bonding appears to be the stabilization of the b_{3g}-HOMO of BQ^{2-} with hydrogen-bonded complex formation. The active MO of BQ^{2-} to the hydrogen bonding is the b_{3u} and b_{1g} n-orbitals localized on the carbonyl oxygen atoms, which is activated enough to accept a proton with two-electron reduction. The activation of the b_{3g}-HOMO of BQ^{2-} as well as the n-orbitals are weakened by the intermolecular n–σ type charge transfer through the hydrogen bond of BQ^{2-} with CH_3OH, as illustrated in Fig. 4. The blue shift in the BQ^{2-} spectra is attributable to the strong stabilization of the b_{3g}-HOMO with the hydrogen-bond formation. A considerable effect of the hydrogen bonding on the π-electron distribution in BQ^{2-} has been found in spite of the negligible π-type charge transfer by hydrogen bonding. It is reasonably understood that the HOMO→LUMO transition for BQH_2 as the most strongly interacted model appears at a wavelength shorter than that of the hydrogen-bonded complex, as shown in Fig. 4. The blue shift of the BQ^{2-} spectra is therefore well explained in terms of the n–σ type charge-transfer interaction from the carbonyl oxygen atom of BQ^{2-} to the hydrogen atom of the alcoholic hydroxy group. This may be considered to be the same spectral behavior as the blue shift in intramolecular charge-transfer bands observed for heterocyclic amine N-oxides[28)] because the excited state of BQ^{2-} is mainly contributed from the $b_{3g} \rightarrow a_u$ intramolecular charge-transfer configuration, as can be seen from Fig. 4.

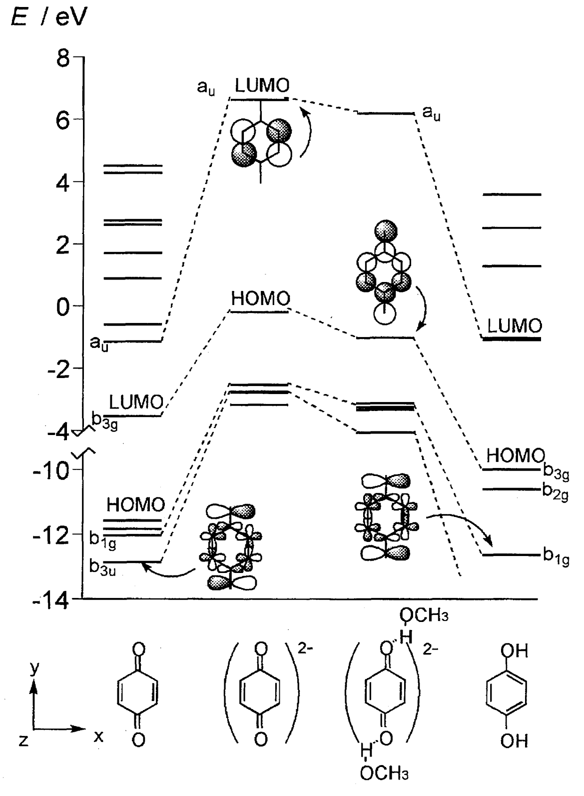

Fig. 4. CNDO/S-CI SCFMO energy levels and the MO illustration relevant to the longest wavelength band of BQ, BQ^{2-} and the hydrogen-bonded complex with CH_3OH, and BQH_2. The axes used for the MO calculations are shown for D_{2h} symmetry.

Conclusion

The method involving rapid circulation of the electrolyzed solution via a photodiode array detector is suitable for the observation of electrogenerated active dianions. We have recorded the electronic spectra of BQ^{2-} and its hydrogen-bonded complex by the use of this method. The hydrogen bonding of BQ^{2-} with CH_3OH allows the spectra of BQ^{2-} to be blue-shifted. The CNDO/S-CI calculations have demonstrated that the band of BQ^{2-} is assigned to the benzenoid ^1L_b band arising from the benzenoid structure altered by two-electron reduction. Hydrogen-bonding of BQ^{2-} is characterized as a blue shift in the BQ^{2-} spectra, resulting from stabilization by the hydrogen bonding involving strong n–σ type charge-transfer interactions. Further inspection of this model can give deeper insight into characterizations of the electrogenerated active dianions and the electron transfers coupled with hydrogen-bonding/proton-transfer interaction of the quinone–hydroquinone redox system.

We thank the Computer Center, Institute for Molecular Science, Okazaki National Research Institutes for the use of the NEC HSP computer and Library Program Gaussian94. This work was supported in part by a Grant-in-Aid for Scientific Research on Priority Areas Nos. 05235240, 06226270, and 07215273 from the Ministry of Education, Science, Sports and Culture.

References

1) B. Uno, A. Kawabata, and K. Kano, *Chem. Lett.*, **1992**, 1017.

2) M. Oyama, A. Takei, and S. Okazaki, *J. Chem. Soc., Chem. Commun.*, **1995**, 1909.

3) N. Gupta and H. Linschitz, *J. Am. Chem. Soc.*, **119**, 6384 (1997).

4) A. Minskey, A. Y. Meyer, R. Poupko, and M. Rabinovitz, *J. Am. Chem. Soc.*, **105**, 2164 (1983).

5) K. Ebata, W. Setaka, T. Inoue, C. Kabuto, M. Kira, and H. Sakurai, *J. Am. Chem. Soc.*, **120**, 1335 (1998).

6) A. Sekiguchi, K. Ebata, C. Kabuto, and H. Sakurai, *J. Am. Chem. Soc.*, **113**, 1464 (1991).

7) A. Sygula and P. W. Rabideau, *J. Am. Chem. Soc.*, **113**, 7797 (1991).

8) X. Zhao, H. Imahori, C. G. Zhan, Y. Sakata, S. Iwata, and T. Kitagawa, *J. Phys. Chem.*, **101**, 622 (1997).

9) J. W. Bausch, P. S. Gregory, G. A. Olah, G. K. S. Prakach, P. v. R. Schleyer, and G. A. Segal, *J. Am. Chem. Soc.*, **111**, 3633 (1989).

10) M. Iyoda, S. Sasaki, F. Sultana, M. Yoshida, Y. Kuwatani, and S. Nagase, *Tetrahedron Lett.*, **37**, 7987 (1997).

11) T. Wakahara, R. Kodama, T. Akasaka, and W. Ando, *Bull. Chem. Soc. Jpn.*, **70**, 665 (1997).

12) C. D. Stevenson and R. M. Fico, Jr., *J. Org. Chem.*, **60**, 5452 (1995).

13) T. Kubota, K. Kano, B. Uno, and T. Konse, *Bull. Chem. Soc. Jpn.*, **60**, 3865 (1987).

14) B. Uno, Y. Matsuhisa, K. Kano, and T. Kubota, *Chem. Pharm. Bull.*, **32**, 1 (1997).

15) A. M. Spreitzer, A. Mannschreck, M. Scholz, G. Gescheidt, H. Spreitzer, and J. Daub, *J. Chem. Res. (S)*, **1995**, 180.

16) J. Q. Charmbers, "The Chemistry of the Quinoid Compounds," ed by S. Patai, Z. Rappoport, Wiley, New York (1988).

17) M. Oyama, K. Nozaki, and S. Okazaki, *Anal. Chem.*, **63**, 1387 (1991).

18) W. R. Heineman, F. M. Hawkridge, and H. N. Blount, "Electroanal Chemistry," ed by A. J. Bard, Marcel Dekker, New York, Basel (1984), Vol. 13, pp. 1—104.

19) B. Uno and N. Okumura, "Recent Research Developments in Pure & Applied Chemistry," ed by S. G. Pandalai, Transworld Research Network, India (1998), Vol. 2, pp. 83—99.

20) B. Uno, K. Kano, T. Konse, T. Kubota, S. Matsuzaki, and A. Kuboyama, *Chem. Pharm. Bull.*, **33**, 5155 (1983).

21) R. L. Ellis, G. Kuehnlenz, and H. H. Jaffé, *Theor. Chim. Acta*, **26**, 131 (1972).

22) G. Kuehnlenz and H. H. Jaffé, *J. Chem. Phys.*, **58**, 2238 (1973).

23) B. Tinland, *Mol. Phys.*, **16**, 413, (1969).

24) N. O. Lipari and C. B. Duke, *J. Chem. Phys.*, **63**, 1748 (1975).

25) C. B. Duke and N. O. Lipari, *J. Chem. Phys.*, **63**, 1758 (1975).

26) P. Jacques, J. Faure, D. Chalvet, and H. H. Jaffé, *J. Phys. Chem.*, **85**, 473 (1981).

27) N. Mataga and K. Nishimoto, *Z. Phys. Chem.* (*Neue Folge*), **12**, 335 (1957).

28) M. Yamanaka, T. Kubota, and H. Akazawa, *Theoret. Chim. Acta*, **15**, 224 (1969).

29) H. H. Jaffé and M. Orchin, "Theory and Applications of Ultraviolet Spectroscopy," John Wiley and Sons, Inc., New York and London (1962), Chap. 9.

30) K. Kimura, K. Yoshinaga, and H. Tsubomura, *J. Phys. Chem.*, **71**, 4485 (1967).

31) B. Uno and T. Kubota, *J. Mol. Struct.* (*Theochem*), **230**, 247 (1991).